E3S Web of Conferences **157**, 01015 (2020) https://doi.org/10.1051/e3sconf/202015701015
KTTI-2019

Reduction of the pull effect of a cylindrical linear synchronous motor

Sergey Shutemov[1], *Evgeniy* Chabanov[1], *Anastasia* Shevkunova[2,*], *Alexander* Shapshal[2], and *Temur* Talakhadze[2]

[1] Perm National Research Polytechnic University, Komsomolsky prospect, 29, Perm, 614990, Russia
[2] Rostov State Transport University, Rostovskogo Strelkovogo Polka Narodnogo Opolcheniya sq., 2, 344038, Rostov-on-Don, 344038, Russia

Abstract. A theoretical and experimental study of the effect of gravity, which occurs in a cylindrical linear synchronous motor between the secondary element and the inductor, was carried out. As a result, the forces of mechanical friction of the secondary element on the inductor are formed, which entails touching the secondary element on the surface of the inductor. An unfavourable result is a weakening of the power force that is working for a cylindrical linear synchronous motor. Two different inductor designs for a cylindrical linear synchronous motor have been studied. When solving this problem, we used an approach based on a combination of the field theory method and the theory of electric circuits. The forces of gravity, friction, and force between the secondary element and the inductor for these structures are determined. Experimentally, it was found that the pull force significantly weakens the working force of the engine. Based on the results obtained, conclusions were drawn about the need to change the design of the inductor. The design change of this element consists in the use of a non-magnetic intermediate centralizer, which is inserted between two sliding bearings located at the ends of each module of a cylindrical linear synchronous motor. Also, changes were made to the design of the magnetic circuit, in which instead of one slot for a three-phase winding system, three symmetrical slots were made, each for its own phase of the three-phase winding. As a result, the magnetic system of the engine in question became axisymmetric. The measures taken to change the design of the engine in question allowed us to dramatically reduce the effect of gravity. As a result, the specific force has increased significantly.

1 Introduction

An electric drive is an indispensable part of any mechanism. Without it, it is impossible to operate machines, household appliances, medical equipment, and various water and gas supply devices. More than 60 % of the electricity generated in the Russian Federation is consumed by electric drives. They allow you to automate and optimize technological processes and increase their efficiency. Modern electric drives differ both in power (from a

* Corresponding author: nastya3051990@mail.ru

fraction of a watt to a dozen MW) and in controls (from conventional switching equipment to electronic computers). They use both low-speed (100 rpm) and high-speed (up to 200,000 rpm) engines, both DC and AC. Currently, there is a tendency to use drives with AC motors. They are more reliable and efficient than DC motors. The Russian Federation is implementing a program to modernize the main equipment in various industries [1–3]. Replacement of last-generation electric drive systems with modern ones. For example, one of the most modern and highly efficient electric motors is a cylindrical linear synchronous (valve) motor (CLVM) [4–8].

Such devices are currently used in many industries: machine tools, transport, robotics, control and protection systems, etc. The introduction of this type of drive, which uses reciprocating motion, will save about 30 % of electricity [9]. For example, in the oil-producing industry, CLVD can be used for rodless oil production from wells with submersible units, which can serve as an alternative to the rocking machines that are widely used today.

The principle of operation of the CRVD is similar to the valve electric machines of rotational motion, the only difference is that the magnetic field moves linearly and it is as if open. High-performance, rare-earth magnets are also located on the secondary element of the CLVD, which structurally correspond to valve motors. This type of machine has better parameters (higher power density and better dynamic characteristics) than a linear asynchronous motor [10, 11].

2 Materials and research methods

When designing the CLVD, the main attention had to be paid to increasing the specific force that moves the secondary element. To implement this task, a calculated search was performed for a rational design of the secondary element and the inductor, which creates the maximum force. As a result of mathematical research, multivariate calculations of a set of curves of static angular characteristics were carried out for various structures of the CLVD. As a result, the design that gives the greatest force was chosen.

The operation of the CLVD is complicated by the existence of the tug effect, which occurs when the secondary element is displaced relative to the inductor axis. As a result, the friction forces between the secondary element and the inductor increase significantly. This is due to the fact that the secondary element and the inductor begin to touch, which leads to a decrease in the force on the secondary element. In addition, there will be severe wear on the surfaces of the inductor and the secondary element. Therefore, the calculation of gravity forces and the implementation of methods to eliminate it is an important task to obtain the necessary characteristics of the CLVD.

3 Results

The design of the CLVD is shown in Figure 1 and it consists of three main parts:

1. Corpus.
2. A cylindrical inductor consisting of ferromagnetic cups with three-phase winding phases laid in them.
3. A secondary element with permanent magnets that performs a reciprocating motion.

Permanent magnets have the following technical characteristics: H_c = 1,400 kA/m, B_r = 1.2 Tl. The inductor consists of cups that make up the teeth and grooves in which the coils of a three-phase inductor are located. The pole division of the motor is τ = 30 mm, and the value of the tooth division t_z = 10 mm.

The coils of each phase of the three-phase winding are connected in series over the length of the inductor. The phases are powered by a connected frequency converter. The phase windings of the cylindrical inductor create a linear traveling magnetic field, the direction and speed of movement of which is changed by the if. The secondary element has a diameter D_p = 53 mm. There is an air gap δ between the secondary element and the inductor, which is 1.5 mm. The secondary element is located symmetrically relative to the axis of the inductor, i.e. their axes are aligned. With this mutual arrangement of the axes of the secondary element and the inductor, the pull force between them is zero.

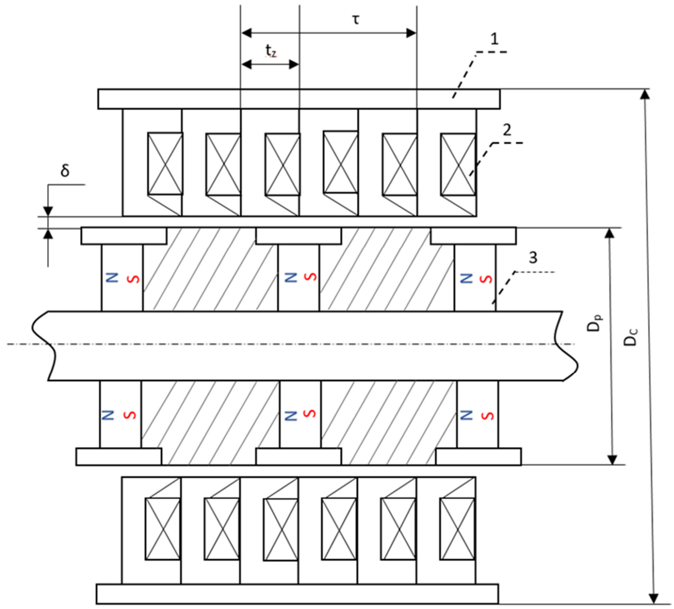

Fig. 1. CLVD in longitudinal section

When the axis of the secondary element is shifted relative to the axis of the inductor, the air gap along the forming diameter becomes uneven, which leads to the appearance of gravity forces directed to the surface of the inductor with the smallest gap. As a result, the secondary element bends under the action of the resulting gravity forces, which as a result leads to even greater unevenness of the working air gap. As a result of radial gravity forces, the unevenness of the working air gap increases, so that the gap on one side in the limit becomes zero, and on the opposite side becomes maximum. Accordingly, the friction forces between the secondary element and the inductor increase significantly, due to their mutual contact, this leads to a decrease in the force force and the appearance of significant wear on the surfaces of the secondary element and the inductor.

Switched reluctance motors with a rotational magnetic field have the same problems. As you know, the smaller the air gap in these machines, the higher the efficiency. However, when the air gap decreases, the radial forces of interaction between the stator and the rotor increase, caused by an increase in the unevenness of the magnetic conductivities between the teeth of the excited phases. To reduce this negative factor, a number of scientists have developed appropriate measures [12–14].

To determine the friction forces that act when the secondary element comes into contact with the inductor, it is necessary to calculate the effect of gravity that occurs in the magnetic system [15]. To do this, divide the diameter of the secondary element and the inductor into 12 sectors, as shown in Figure 2.

The angle n is counted from the Y axis and divided into 6 angular values: 0, 30, 60, 90, 120, 150 degrees that define the sectors of the inductor breakdown. According to Maxwell's equation, the force of attraction between the inductor and the secondary element in the gap depends on the magnitude of the magnetic induction in each sector along the circumference of the inductor's diameter.

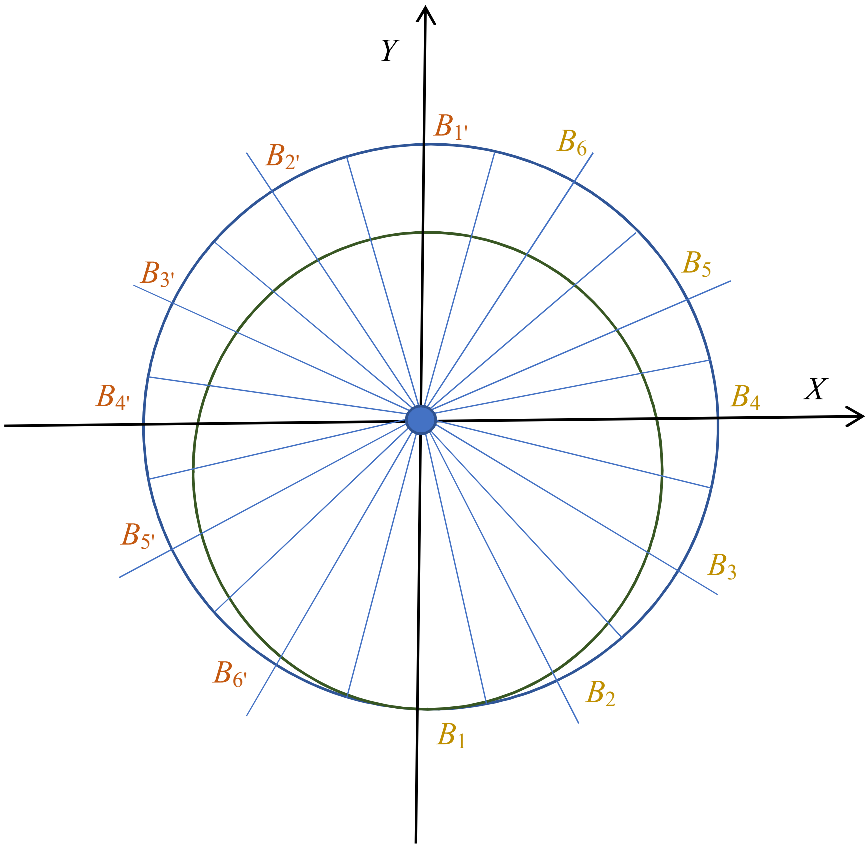

Fig. 2. Breakdown of the diameter of the magnetic system of the CLVD into sectors

$$F_{Bn} = \frac{B_c \times B_c \times S}{2\mu_0}, \tag{1}$$

where $S = mi \times \imath = 13{,}4 \cdot 10^{-3}$ - area of each sector.

The forces acting in each sector are directed in different directions, so according to the system of equations, the resulting forces for the sectors are equal

$$\begin{gathered} F_{C1} = F_{B1} - F_{B1'}; \quad F_{C2} = F_{B2} - F_{B2'}; \\ F_{C3} = F_{B3} - F_{B3'}; \quad F_{C4} = F_{B4} - F_{B4'}; \\ F_{C5} = F_{B5} - F_{B5'}; \quad F_{C6} = F_{B6} - F_{B6'}. \end{gathered} \tag{2}$$

Force component of the Fc section along the axis

$$F_{yn} = F_{cn} \times \cos(\alpha). \tag{3}$$

As a result, we find the force of gravity F_m CLVD, which occurs along the y axis in accordance with the equation

$$F_m = \sum_1^n F_{yn}. \tag{4}$$

The obtained values of the values of the forces of gravity of the secondary element of the CLVD by sector are presented in Table 1.

As a result of magnetic calculations, we obtained the value of the tension force along the *y* axis, and found that it must be taken into account to determine the friction forces, since it is significant in magnitude.

Table 1. Results of calculation of the value of the forces of gravity of the CLVD.

The axis of the sector	Magnetic induction at the ends of the axes, B_c, Tl		Angle of an axes α, degree	Forces at the ends of the axes, N		The result of the force on the axes, F_{cn}, N	The result of the force on the axis Y, F_{yn}, N
	n	n'		F_{Bn}	$F_{Bn'}$		
$B1$-$B1$'	0.836	0.615	0	3,730	2,017	1,712.4	1,712.4
$B2$-$B2$'	0.794	0.628	30	3,362	2,175	1,187	1,057.5
$B3$-$B3$'	0.756	0.660	60	3,048	2,323	725	426
$B4$-B4'	0.710	0.710	90	2,020	2,020	0	0
$B5$-$B5$'	0.660	0.756	120	2,323	3,048	725	426
$B6$-$B6$'	0.628	0.794	150	2,175	3,362	1,187	1,057.5
Итого						F_t, N	4,679.4 N

Calculations have shown that the value of the tension force is almost equal to 4.7 kN, from which it is possible to determine the value of the friction force of the secondary element on the inductor. Such a significant amount of tension leads to a deflection of the secondary element, which exceeds the value of the air gap. As a result, there are significant friction forces, the power force on the secondary element falls.

4 Consideration

Also, the resulting magnetic asymmetry of the inductor design can lead to a significant increase in the tug effect. This fact is associated with the appearance of asymmetry of the radial magnetic flux between the secondary element and the inductor, due to the presence of only one slot for laying three-phase connecting windings. As a result, there is an asymmetry of the radial magnetic flux between the secondary element and the inductor, resulting in an additional force of gravity. The asymmetry of the radial magnetic flux causes the secondary element to be attracted to the inductor, which creates additional mechanical friction that reduces the power force.

In order to eliminate this harmful phenomenon, an additional intermediate centralizer was added to the CLVD module to reduce the amount of friction that occurs and to center the secondary element relative to the inductor axis. The diameter of the centralizer is selected from the condition $D_C < (D_P + 2\delta)$ and $D_P < D_C$ so that the gap between the secondary element and the inductor is limited by the centralizer during operation of the centralizer.

It was also changed to an axisymmetric inductor design to significantly reduce the effect of gravity. The design of the inductor channel was changed to accommodate the ends of the three-phase winding. Instead of one channel for all three phases, three separate channels were made, one for each phase, with a spatial displacement of 120 degrees in accordance with Figure 3.

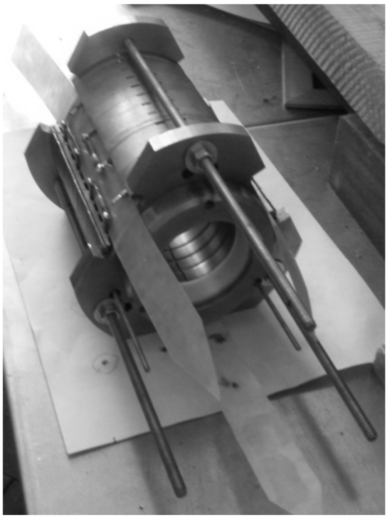

Fig. 3. Inductor with three symmetrical slots

This design change leads to a more uniform distribution of the radial magnetic flux and leads to the elimination of the magnetic flux asymmetry, which reduces the magnitude of the gravity effect. The use of an axisymmetric inductor design made it possible to achieve a significant increase in the power force by reducing the magnitude of the gravity forces, and as a consequence, the friction forces. This design solution is necessary for a more uniform distribution of the radial magnetic field, which allowed to achieve an increase in the force of the secondary element by 1kN.

When determining the force on the secondary element CLVD note that it is the difference between the electromagnetic force generated by the inductor, and the secondary friction element in sliding bearings. Figure 4 shows the data experimentally measured force forces on the secondary element depending on the motor current for two variants of the design of the CVDC inductor (*F* and *F'*).

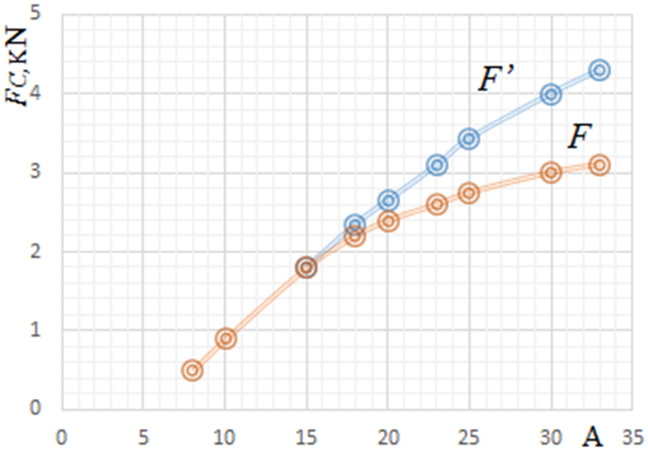

Fig. 4. Power force on the secondary element for two structures

The difference in the measured force forces for two designs of inductors is 1 kN, with a current of 30 A. it should be taken into account that a significant difference in the forces F and $F^{'}$ occurs only at currents of more than 16 A.

An experimental study related to the problem of gravity allowed us to solve a number of important theoretical and practical problems, to develop solutions to eliminate this harmful effect by changing the design of the Central air pump. As a result, it was possible to achieve the necessary power efforts.

5 Conclusion

As a result of theoretical and experimental studies of the effect of gravity, we found out the degree of its influence on the work of the CLVD. The obtained values of the force of gravity and power force for the two considered structures of the CLVD allowed us to determine the friction forces between the secondary element and the inductor. It was found that the value of the friction force between the secondary element and the inductor is significant, and it must be taken into account. Based on the analysis of the measured and calculated forces of gravity and friction, it was concluded that it is necessary to use a non-magnetic centralizer, which allows reducing the amount of friction forces. This helps to center the secondary element relative to the inductor, which eliminates their contact. To eliminate the harmful effect of gravity, the inductor design was also changed. The design of the inductor slots was changed, in which three slots were made to accommodate the three-phase winding conductors. As a result, the inductor design became axisymmetric. This design change is necessary for a more uniform distribution of the radial magnetic field. Changing the design of the CLVD inductor to an axisymmetric one made it possible to achieve an increase in the power force of the secondary element by 1kN.

References

1. L. Proskuryakova, S. Filippov. Energy technology Foresight 2030 in Russia: an outlook for safer and more efficient energy future, **75**, 2798-2806 (2015), doi: 10.1016/j.egypro.2015.07.550
2. A. Karandaev, V. Khramshinb, R. Khramshinb, I. Barankova. Conceptual Area of Development of Power Saving Thyristor Electric Drives of Rolling Mills, **150**, 3-10 (2016), doi: 10.1016/j.proeng.2016.07.272
3. L. Proskuryakova. Foresight for the ‘energy’ priority of the Russian Science and Technology Strategy, **26**, 100378 (2019), https://doi.org/10.1016/j.esr.2019.100378R
4. Y. Kwon, H. Kim, S. Baik, E. Lee, K. Ryu. Performance test of a 1MW class HTS synchronous motor for industrial application, **468**, 2081–2086 (2008), https://doi.org/10.1016/j.physc.2008.05.249
5. Raúl-S. Muñoz-Aguilar, Arnau Dòria-Cerezo, Enric Fossas. Extended SMC for a stand-alone wound rotor synchronous generator, **84**, 25-33 (2017), https://doi.org/10.1016/j.ijepes.2016.04.052
6. Kyo-Beum Lee, Hye-Ung Shin, Yeongsu Bak. Chapter 11-Basic Control of AC Motor Drives, 301-329 (2018), https://doi.org/10.1016/B978-0-12-805245-7.00011-1
7. U.Thakar, V. Joshi, U. Mehta, V.A.Vyawahare. Chapter 18 – Fractional-Order PI Controller for Permanent Magnet Synchronous Motor: A Design-Based Comparative Study, 553-578 (2018), https://doi.org/10.1016/B978-0-12-816152-4.00018-2
8. C. Xiang, F. Liu, H. Liu, L. Han, X. Zhang. Nonlinear dynamic behaviors of permanent magnet synchronous motors in electric vehicles caused by unbalanced magnetic pull, **371**, 277-294 (2016), https://doi.org/10.1016/j.jsv.2016.02.015

9. N. Shevkunov, A. Zhigunova, A. Shevkunova. Modeling parameters of the production project, **560** (2019), doi: 10.1088/1757-899X/560/1/012043
10. Guan Xiao-cun, Lei Bin, Li Zhi-yuan, Zhao Ran. Research on Performance High-speed Multi-stage Cylinder Linear Induction Motor, **16**, 1904-1912 (2012), doi:10.1016/j.egypro.2012.01.291
11. Hongwen He, Nana Zhou, Chao Sun. Efficiency decrease estimation of a permanent magnet synchronous machine with demagnetization faults, **105**, 2718-2724 (2017), doi: 10.1016/j.egypro.2017.03.922
12. A. Petrushin, E. Miroshnichenko, M. Tchavychalov. Increasing the Field Reliability of Traction Switched Reluctance Motor Drive of Railway Rolling Stock. Journal of Engineering and Applied Sciences, **10 (5)**, 102–106, 2015
13. H. Torkaman, E. Afjei. Magnetostatic Field Analysis Regarding The Effects Of Dynamic Eccentricity In Switched Reluctance Motor. Progress In Electromagnetics Research, **8**, 163-180 (2009)
14. A. Petrushin, M. Tchavychalov, E. Miroshnichenko. The Switched Reluctance Electric Machine with Constructive Asymetry. International Journal of Power Electronics and Drive System (IJPEDS), **6 (1)**, 86-91, 2015
15. Yoo Jaeun, Lee SangMoo, Jung YeHyun, Lee Jaeyoung, Oh SangSoo. Calculations of AC current losses and AC magnetic losses from the scanning Hall probe measurements for a coated conductor, **468 (31)**, 160–168 (2008), https://doi.org/10.1016/j.physc.2007.11.002